frontiers | Frontiers in Energy Research

TYPE Original Research
PUBLISHED 08 January 2024
DOI 10.3389/fenrg.2023.1342811

OPEN ACCESS

EDITED BY
Zhengmao Li,
Aalto University, Finland

REVIEWED BY
Bin Gou,
Southwest Jiaotong University, China
Heling Yuan,
Nanyang Technological University, Singapore

*CORRESPONDENCE
Liang Zhang,
xiaozhanghit@163.com

RECEIVED 22 November 2023
ACCEPTED 13 December 2023
PUBLISHED 08 January 2024

CITATION
Wang B, Wang F, Zou Y, Fang S, Luan H and Zhang L (2024), Proposed multi-signal input fault diagnosis of wind turbine bearing based on glow model. *Front. Energy Res.* 11:1342811. doi: 10.3389/fenrg.2023.1342811

Proposed multi-signal input fault diagnosis of wind turbine bearing based on glow model

Bin Wang[1], Fei Wang[1], Yunbo Zou[1], Shunshun Fang[1], Hanzhang Luan[2] and Liang Zhang[2]*

[1]State Power Investment Corporation Anhui Electric Power Co Ltd., Hefei, Anhui, China, [2]School of Electrical Engineering, Northeast Electric Power University, Jilin, Jilin, China

In the fault diagnosis, the problem of insufficient fault samples and unbalanced number of fault category samples can occur. In this paper, we used Glow model to supplement the number of wind turbine bearing fault samples to enhance the diagnosis accuracy when fault samples are insufficient and the number of fault category samples is unbalanced. Meanwhile, we established a multi-input fault diagnosis model to achieve multi-location and multi-category fault diagnosis, and constructed some experimental under different scenarios. We took into account the noise interference in the actual operation and conducted comparison experiments under different scenarios, and the experimental results verified the new algorithm had good fault diagnosis effect.

KEYWORDS

deep learning, flow-based models, image processing, wind turbine fault diagnosis, glow model

1 Introduction

In today's industrial and civil domains, the utilization of networked autonomous systems, including power systems and mobile sensor networks, has emerged as an indispensable asset (Fang et al., 2023). Wind energy has been widely used and has wide developing prospect (Shiyao et al., 2023). Under the background of China's goal of carbon peak and carbon neutrality, the wind power industry has even greater room for development (Heling and Yan, 2020). According to relevant statistics, the gross capacity of global wind power will reach 837 GW in 2021, which is 93.6 GW more than in 2020, indicating that the ratio of wind power generation in the gross generation will be further increased.

With the continuous improvement of installed capacity, the operation maintenance of wind generators has attracted wide attention. Because of the harsh operating condition, the wind generator causes frequent failures, but their operation and maintenance are not convenient. Compared with other components in the driving chain of wind generator, the bearing is one of the important parts with high failure probability, and its operating state often immediately influences the work of the entire machine (Chen et al., 2016).

Vibration analysis has been the most popular method for mechanical failure diagnosis. The traditional method based on vibration signal analysis mainly extracts fault features from the gathered signals and then uses different algorithms to classify the fault features. Bearing vibration signals usually exhibit time-varying, nonlinear and non-smooth signals (Song et al., 2022) and are easily disturbed by noise during the acquisition process, which leads to difficulties in extracting fault features for different fault scenarios of bearings. To address this problem, many scholars have achieved a series of research results. To address the difficult

trouble of extracting fault feature accurately, reference (Yongsheng et al., 2022) proposed a feature extraction method of adaptive empirical wavelet transform (AEWT) with singular value decomposition (SVD), and combined with kernel limit learning machine (KELM) to achieve failure detection. Reference (Liu et al., 2021) applied acoustic emission (AE) analysis to filter acoustic emission signals and extract weak fault signals to achieve failure detection of industrial-scale slow wind turbine blade bearings. Reference (Zhang et al., 2020) present a weak fault diagnosis method combining variational modal decomposition (VMD) and maximum correlated kurtosis deconvolution (MCKD), which can adaptively improve the impact com-ponents in the weak fault. Reference (Zheng et al., 2019) proposed a fault feature extraction method of the vulnerable parts based on variational mode decomposition, and used the deep belief net-work to warn the fault. In the reference (Wang et al., 2021), Adaptive Chirp Mode Decomposition was ap-plied to the bearing fault diagnosis, and the transient frequency selection strategy guided by the l-kurtosis fluctuation spectrum and the weighting factor determination strategy guided by the cuckoo search algorithm (CSA) were used for the defect identification of bearings. The realization of noise reduction, filtering, feature extraction and other processes in traditional fault diagnosis methods depends on specialized knowledge and la-bour power. The quality of extracted features may affect the effectiveness of failure detection. And when complex faults are found, feature extraction may be difficult. With the ad-vent of the information age and the advancement of computer technology, the application of artificial intelligence deep learning has gradually replaced the traditional method of manually extracting fault features, saving a lot of manpower and slowly weakening the importance of expert experience.

The emergence of deep learning algorithms has provided new ideas for fault diagnosis. Compared with traditional methods, deep learning can achieve “end-to-end” fault diagnosis. In the case of limited fault samples, the fault diagnosis methods based on deep learning algorithm have greater advantages. For this problem, many scholars have achieved a series of research results. Reference (Pu et al., 2020) proposed a deep enhanced fusion network, which uses experimental vibration data for gearbox fault diagnosis. Reference (Yu et al., 2021) proposed a new fast deep graph convolutional network technique for wind turbine gearbox fault diagnosis. Reference (Su et al., 2022) present a modified gear failure detection method based on generative adversarial networks for unbalanced data sets with better capability in the generation, classification and diagnostic accuracy of fault features under unbalanced data sets. Reference (Zhang et al., 2021) proposed signal augmented self-learning learning network for generator fault diagnosis with good robustness in noisy operating environment. Reference (Huang et al., 2020) proposed an improved label-noise robust auxiliary classifier generative adversarial network driven by the limited data, which is able to keep good diagnostic efficacy of main bearing failure detection in different scenarios.

At present, deep learning algorithms have been increasingly used in failure detection. In terms of fault sample generation, VAE and GAN are more applied, and flow model is less applied. We have used VAE and GAN models in their previous studies to achieve multi-category bearing fault diagnosis using a multi-signal fusion approach. In this study, based on the previous research, different models and simultaneous input of multiple signals are used to achieve multi-category bearing fault diagnosis.

In the actual operation of the wind generator, the probability of bearing failure is relatively low and the probability of each category of failure is not the same. The number of samples that can be collected for each type of fault is different and limited, so in wind generator bearing failure diagnosis, the problem of insufficient fault samples and unbalanced number of fault category samples will occur. To address these problems, the following contributions are made in this study.

(1) The number of fault samples is supplemented by using the Glow model to learn the fault characteristics of each bearing fault category to generate fault samples.
(2) A multi-input bearing fault diagnosis model is established by convolutional neural network to achieve effective diagnosis of multi-location and multi-category bearing faults.
(3) After obtaining the fault samples generated by the GLOW model, we construct the fault sample sets under different scenarios, considering the insufficient samples, unbalanced number of samples and noisy scenarios in actual operation. The diagnostic accuracy of these sample sets in the multi-input fault diagnosis model can prove the effectiveness of the proposed algorithm.

1.1 Flow-based models

The common sampling-based generative models have three types: Variational Auto-encoder (VAE), Generative Adversarial Network (GAN), and Flow-Based Models (Zhang et al., 2021). VAE can naturally generate low-dimensional space, approximate the sample distribution, and generate new samples easily. However, the gradient is difficult to calculate in the VAE model, and it can only optimize the lower boundary line of the edge likelihood function. The performance is generally inferior to that of GAN. GAN is good at generating samples, sampling to get new samples is easy, but the training of the model is difficult and the stability is poor. GAN cannot be used to get the sample distribution, and it is easy to have model collapse. Compared with the above two models, Flow-based Models can get the sample distribution and also the useful hidden space, and the training is very easy.

Flow Based Models are probabilistic generative models based on reversible transformations in which both sampling and density evaluation can be valid and accurate. The probabilistic generative model is a model used to learn the distribution of random variable X from a pile of sample data $\{x_i\}_{i=1}^{N}$.

There are real sample data X and random variable Z, where Z obeys the known simple prior distribution π(z), and the sample data X obeys the complex distribution p(x). If there is a transformation function f that satisfies the mapping from Z to X.

$$\boldsymbol{f}: \boldsymbol{Z} \rightarrow \boldsymbol{X}$$

Every sampling point in $\pi(z)$ have a corresponding sample point in $p(x)$ in order to obtain generated sample. Although most distributions in the real world are more complex than Gaussian distributions, Gaussian distributions are often used in latent variable

generation models to calculate derivatives more easily and effectively.

The flow model generation process can be defined by the following formula (Dinh et al., 2014):

$$z \sim \pi(z)$$
$$x = g_\theta(z)$$

In the above equation, z is the hidden variable; $\pi(z)$ is the sample distribution of the hidden variable z; g_θ is an invertible function, so the hidden variable z can be interpreted as $z = f_\theta(x) = g_\theta^{-1}(x)$, where f_θ consists of a series of transformed functions: $f_\theta = f_1 \circ f_2 \circ \ldots \circ f_K$. The relationship between x and z can be expressed as:

$$x \overset{f_1}{\rightarrow} h_1 \overset{f_2}{\rightarrow} h_2 \cdots \overset{f_K}{\rightarrow} z$$

This sequence of reversible transformations is known as the Normalizing Flow (Rezende and Mohamed, 2015). In Normalizing Flow, the prior distribution $\pi(z)$ of random variables Z usually chooses Gaussian distribution, so that the model can be used for better and more powerful distribution approximation. Normalizing Flow can transform simple distribution into complex distribution by using a series of reversible transformation functions, and then the new variables are repeatedly replaced based on the variable substitution theorem, and finally we can get the probability distribution of the target variable. From the above equation, the model probability density function for a given sample data x can be expressed as:

$$\log p_\theta(x) = \log p_\theta(z) + \log\left|\det\left(\frac{dz}{dx}\right)\right|$$
$$= \log p_\theta(z) + \sum_{i=1}^{K} \log\left|\det\left(\frac{dH_i}{dH_{i-1}}\right)\right|$$

It is easier to obtain the exact log-likelihood of the input through the Normalizing Flow. The training loss function of the generation model is the negative log-likelihood on the input data set:

$$L = -\frac{1}{D}\sum_{i=1}^{D} \log p(X_i)$$

The generator of the flow model is subject to some mathematical constraints, which leads to its own expression ability may be insufficient. Therefore, it is generally necessary to stack multi-layer networks to get a generator, which is also the origin of the name ' flow model '. Because it requires the same dimension of input and output, the calculation is very large.

1.2 Glow model

The Glow model is a simple generative normalized flow model using reversible 1 × 1 convolution, improving on NICE (Dinh et al., 2014) and Real NVP (Dinh et al., 2016). The Glow model consists of a series of repetitive layers named scale. Each scale consists of a squeeze function and a flow step, and each flow step contains three parts, Activation Normalization Layer (ActNorm Layer), 1 × 1 Convolution Layer and Affine Coupling Layer (van de Schaft and van Sloun, 2021), and the flow step is followed by a splitting function. Figure 1 shows one step of Glow.

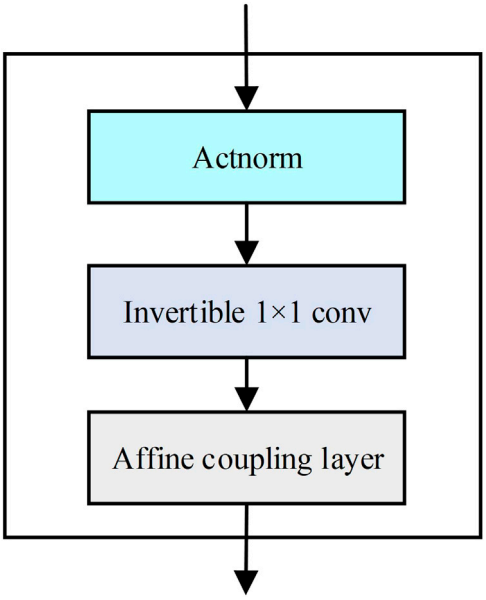

FIGURE 1
One step of Glow.

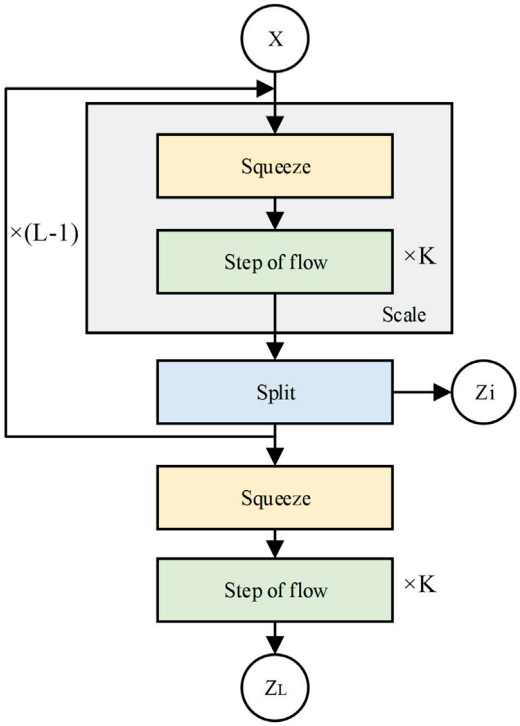

FIGURE 2
Multi-scale architecture.

Figure 2 shows the multi-scale structure. The splitting function divides the input into two equal parts in the channel dimension. One-half goes to the subsequent layer and the other half goes to the

TABLE 1 The fault sample set.

Serial number	Fault category	Fault location	Damage diameter (inches)
1	normal		
2	fan end fault	inner ring	0.007
3			0.014
4			0.021
5		rolling element	0.007
6			0.014
7			0.021
8		outer ring	0.007
9			0.014
10			0.021
11	drive end fault	inner ring	0.007
12			0.014
13			0.021
14		rolling element	0.007
15			0.014
16			0.021
17		outer ring	0.007
18			0.014
19			0.021

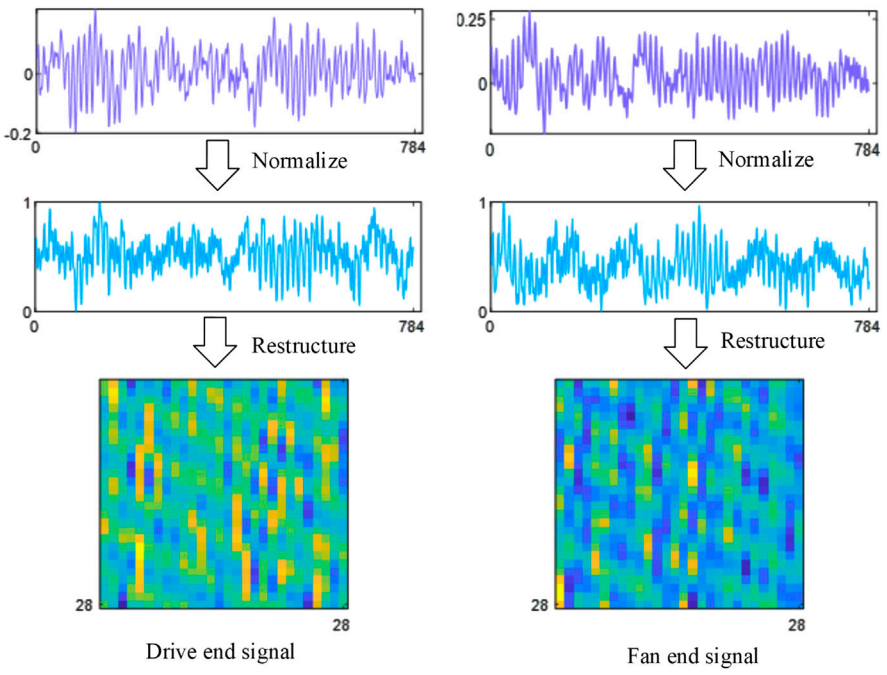

FIGURE 3
The normalization and reshaping process of the data.

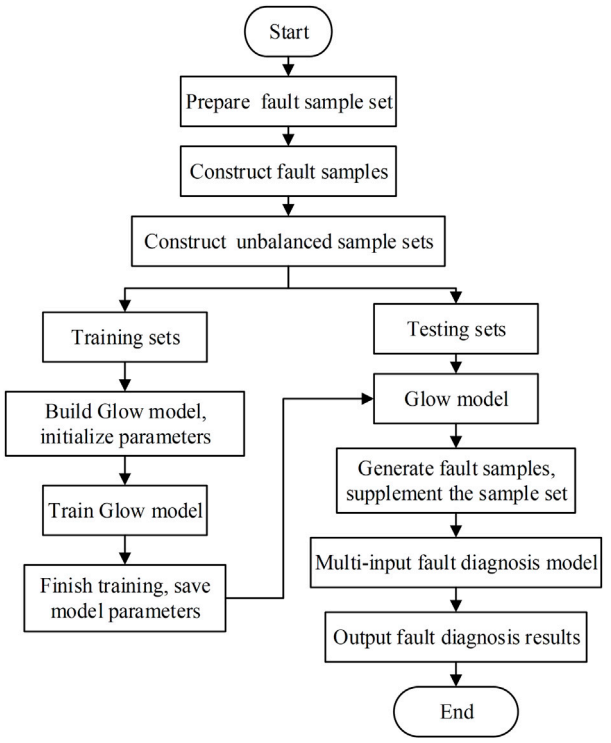

FIGURE 4
Fault diagnosis process.

loss function. The splitting is done to reduce the effect of gradient disappearance, which occurs when the model is trained in an end-to-end mode.

The ActNorm Layer is used for activation normalization, similar to batch normalization, which uses the scale and deviation parameters of each channel to affine transform the activation. Initializing these parameters makes the posterior behavioral actions of each channel have zero mean and unit variance for a given initial small batch of data. This is a form of the data-dependent initialization (Salimans and Kingma, 2016). After initialization, the scales and biases are considered as regular trainable parameters independent of the data.

The 1×1 invertible convolution layer is used to invert the ordering of the channels, where the weight matrix is initialized to a random rotation matrix and the number of input and output channels of the convolution layer is the same. The overall computation can be simplified by the simplified computation of the matrix.

The affine coupling layer creates a flexible and easy-to-handle bijection function by accumulating a series of simple bijections. In each simple bijection, some input vector is updated by utilizing a simple inverse function, but it rests with the other input vector in a complex way. The affine coupling layer can be divided into three parts: Zero initialization, Split and concatenation, and Permutation.

1.3 Advantages of glow model

Compared to other deep learning generative models, the Glow model has the following advantages:

(1) Exact potential variable inference and log-likelihood evaluation. In reversible generative models like Glow, the exact inference of potential variables can be achieved without approximation, and the exact log-likelihood of the data can also be optimized.
(2) Flow-based generative models such as Glow are effective in parallelizing inference and synthesis.
(3) There are potential spaces useful for downstream tasks, and the hidden layers of autoregressive models have unknown marginal distributions (Kingma and Dhariwal, 2018), making it difficult to perform effective data manipulation on them.
(4) A certain amount of memory is required to compute the gradient in reversible neural networks.

2 Multi-signal input fault diagnosis model for wind turbine bearings

2.1 Fault sample construction

The wind generator bearing mainly consists of outer ring, inner ring, rolling element and cage. One end of the bearing is connected to the wind turbine blade, and the other end is connected to the wind turbine drive system. The inner ring is connected to the shaft, and the outer ring is connected to the cage. The rolling element is the key component of the bearing rotation. Therefore, the inner ring, outer ring and sphere may fail. During operation, the main bearing area is easily affected by external factors and causes failure. This experiment data is from of the bearing data center of Case Western Reserve University (CWRU) (Loparo, 2012). The experimental sample set was selected from the drive end and fan end bearing failure data at 12 K sampling frequency with a motor load of 2 hp and an approximate motor speed of about 1750 r/min, and the collected data contained fan and drive end vibration data. The faults were classified into 19 categories according to the fault category (normal, fan end fault, drive end fault), fault location (inner ring, rolling element, outer ring) and damage diameter (0.007 inches, 0.014 inches, 0.021 inches), as shown in Table 1.

Because the design of one-dimensional convolution network is difficult and easy to lead to over-fitting (Xiao et al., 2019), this paper chooses to convert the one-dimensional timing signals from the fan end and the drive end of the wind turbine bearing into twodimensional image signals for fault sample generation and fault diagnosis through a two-dimensional convolutional network, respectively. Based on the bearing rotation speed and sampling frequency, approximately 411 points can be sampled for each rotation of the bearing. In order to ensure the integrity of information and the effectiveness of fault features and to mine more detailed features, 784 sampling points in about 2 rotation cycles are selected as the pixel points of the 2D grayscale image with the image format of 28×28. The original 1D time-domain signal needs to be normalized before the sample construction. The data processing is shown in Figure 3.

2.2 Multi-signal input fault diagnosis model

For the purpose of realizing multi-category bearing fault diagnosis, this paper presents a new fault diagnosis model for

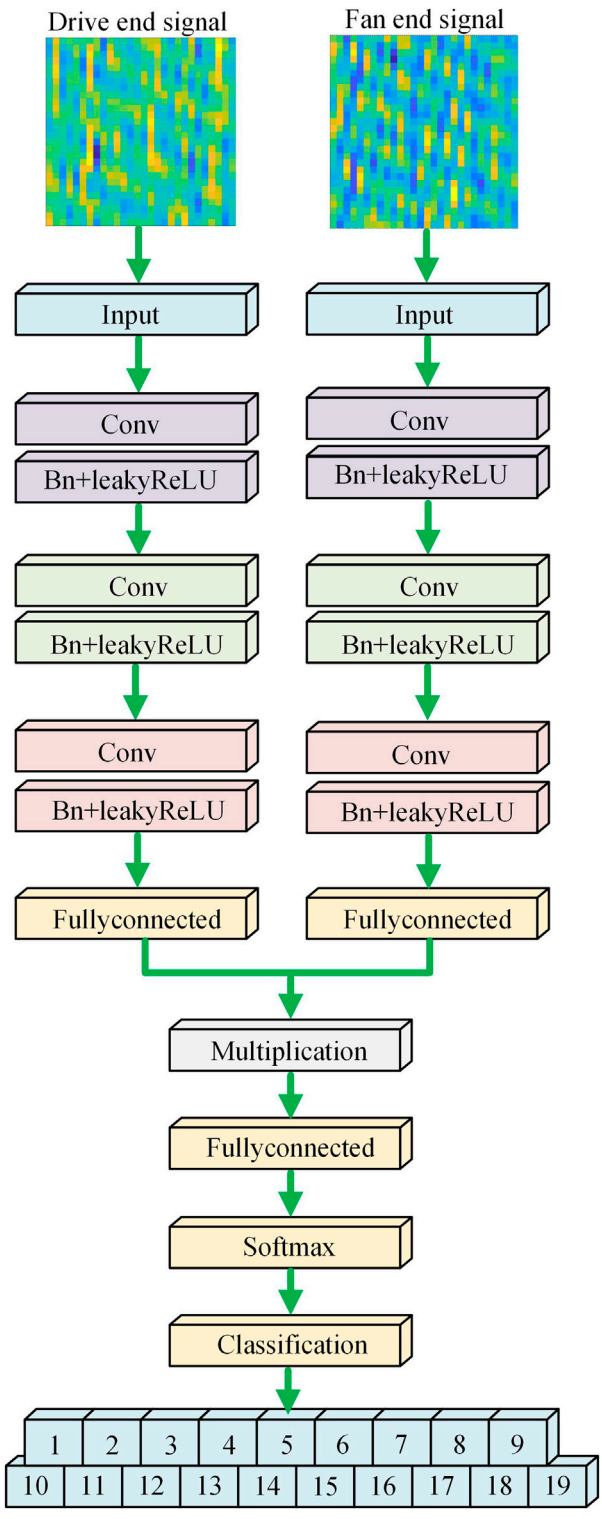

FIGURE 5
Multi-signal input fault diagnosis model.

wind turbine bearings with multiple image inputs based on convolutional neural networks. The convolution layer of the convolutional neural network can extract the local part of the image, which greatly improves the accuracy of the model. For adding some noise to the data set or disturbing the input to a certain extent, the convolutional neural network can still perform good recognition and analysis. Moreover, the convolutional neural network can effectively reduce the over-fitting of the model, thereby improving the generalization ability of the model. Convolutional neural network has the advantage of fast convergence of back propagation algorithm, and can train the depth model in a short time. In general, convolutional neural networks have many advantages. For

TABLE 2 Quality evaluation of generated fault samples.

Noise intensity (dB)		MMD	PSNR	FSIM
0	drive end signal	0.0915	8.0023	0.9612
	fan end signal	0.1005	7.9099	0.9492
20	drive end signal	0.0985	7.6673	0.9746
	fan end signal	0.1002	7.6032	0.9590
30	drive end signal	0.0989	7.8730	0.9632
	fan end signal	0.1060	7.7428	0.9505
40	drive end signal	0.0891	7.6675	0.9624
	fan end signal	0.1005	7.8679	0.9497

TABLE 3 Comparison of sample generation quality.

Model		MMD	PSNR	FSIM
GLOW	Drive End	0.0915	8.0023	0.9612
	Fan End	0.1005	7.9099	0.9492
GAN	Drive End	0.1099	7.2302	0.9726
	Fan End	0.1109	7.0293	0.9492
VAE	Drive End	0.1059	6.3795	0.9605
	Fan End	0.1223	6.0977	0.9301

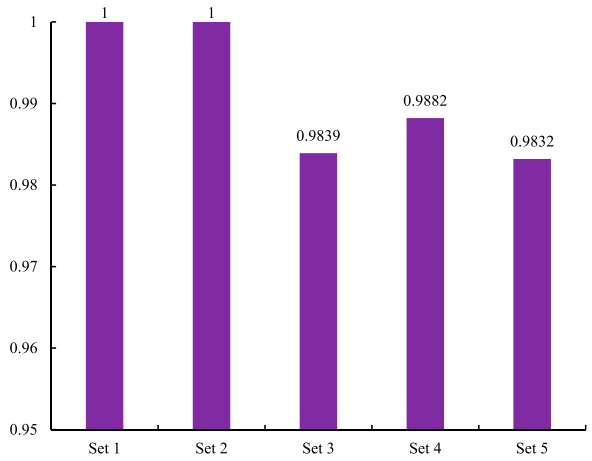

FIGURE 6
Fault diagnosis results for different sample sets under sample imbalance scenario.

TABLE 4 Small sample set.

Sample set	The number per fault class	The total number of samples
6	1,000	19,000
7	900	17,100
8	800	15,200
9	600	11,400
10	400	7,600

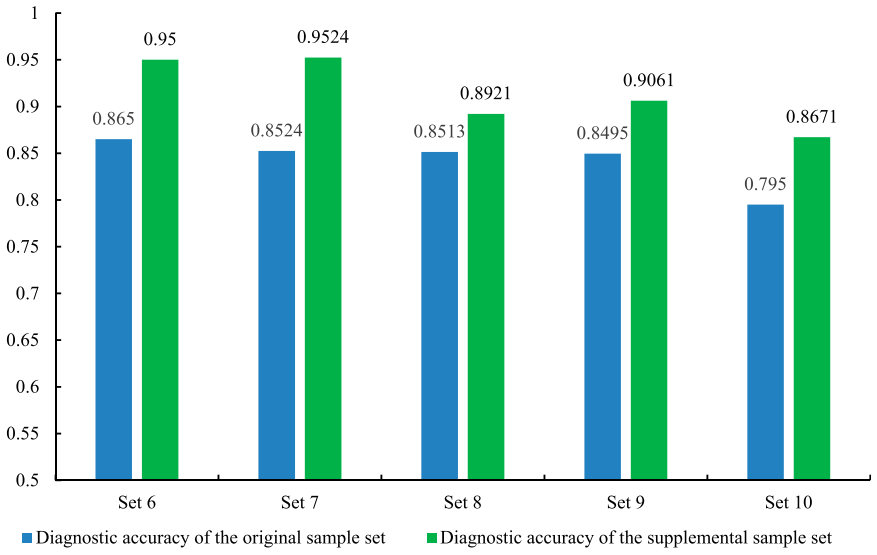

FIGURE 7
Fault diagnosis results for the original sample set and the supplemental sample set in the sample shortage scenario.

TABLE 5 Unbalanced sample set.

Sample set	Unbalanced sample classes	The total number of samples
1		38,000
2	2, 12	36,000
3	3, 7, 13, 15	34,000
4	4, 6, 9, 11, 16, 18	32,000
5	2, 5, 8, 10, 11, 14, 17, 19	30,000

image, audio and other fields, the advantages of convolutional neural networks are more obvious. However, convolutional neural networks also have their limitations, such as large amount of model calculation, complex training data, etc., so in practical applications, it is necessary to select the appropriate model according to the actual situation.

The single input fault diagnosis model can only diagnose one position of the wind turbine bearing fault. However, the multi-signal input fault diagnosis model can learn the fault features of multiple image inputs to achieve the function of fault diagnosis. The model can diagnose the faults of multiple positions of the wind turbine bearing according to the vibration data of multiple different positions. In contrast, the multi-signal input fault diagnosis model can help improve the convenience of wind turbine operation and maintenance, effectively save operation and maintenance costs, and improve the economic benefits of wind farms.

Figure 4 depicts the structure of the multi-image input fault diagnosis model. The model input is 2 grayscale images of size 28 × 28, each input is convolved by multiple convolution layers, and the output is connected to a fully connected layer. The model uses a phase multiplication layer to multiply the inputs from two fully

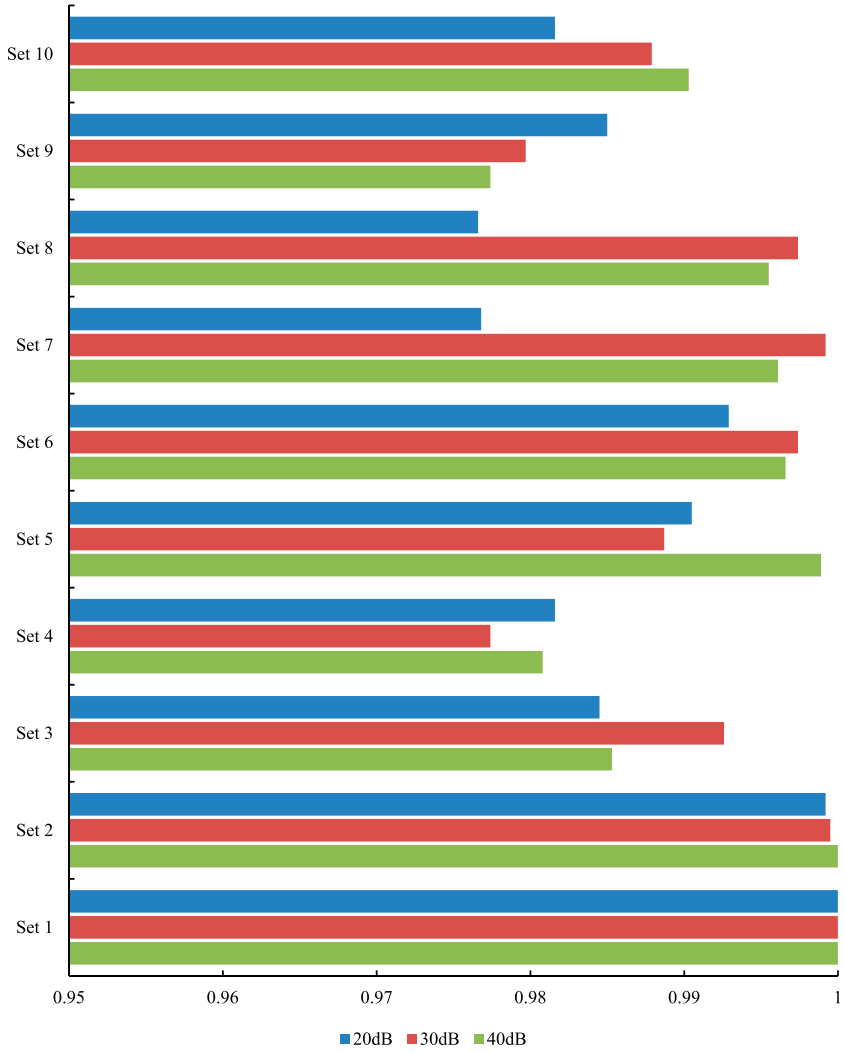

FIGURE 8
Fault diagnosis results of different sample sets under different noise intensity.

connected layers. The model output is a classification layer with softmax activation function.

In this study, the two-dimensional images of vibration signals at the fan end and the drive end of the wind turbine bearing are input into the multi-input fault diagnosis model. Considering different scenarios in the wind generator operation, the fault sample sets under different scenarios are constructed, and the multi-input fault diagnosis model is used to achieve multi-category bearing fault diagnosis. Figure 5.

2.3 Algorithm flow

The process of the multi-signal input fault diagnosis based on Glow model is as follows:

(1) Convert 2 sets of normalized original 1D signals into 2D grayscale image.
(2) Construct the sample sets and divide the training data and test data.
(3) Train the Glow model with the two sets of input signals in the training data.
(4) Complement the fault samples by Glow model, and form the fault sample sets under different scenarios by generating samples and real samples.
(5) Train the multi-input fault diagnosis model.
(6) Input the fault sample sets under different scenarios into the multi-input fault diagnosis model and get the diagnostic results. The algorithm flow is shown in Figure 5.

3 Case analysis

The study firstly verifies the model fault sample generation performance. Meanwhile, considering the problems of insufficient fault samples, unbalanced number of fault category samples, and

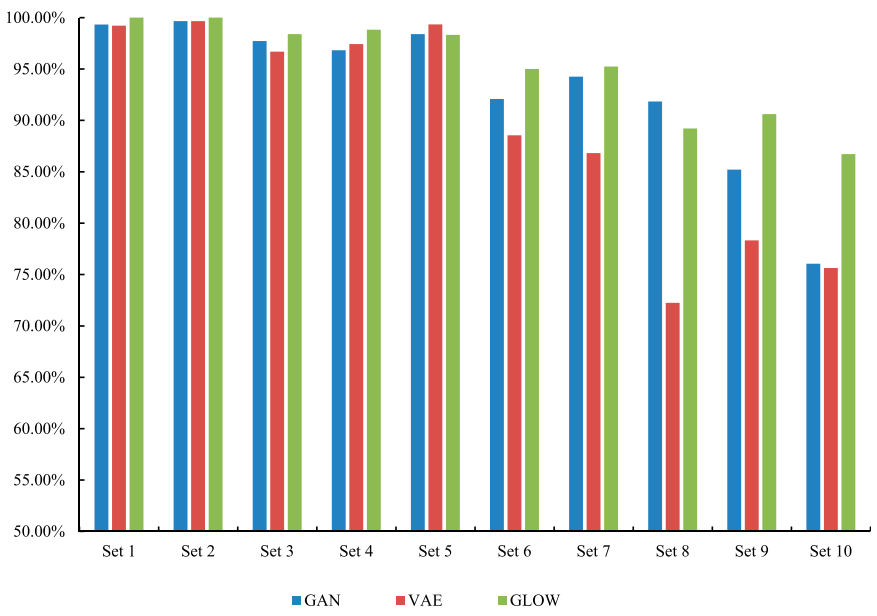

FIGURE 9
Fault diagnosis accuracy of supplemented sample sets with different deep generative models.

noise interference in fault diagnosis in actual operation of wind turbines, comparison experiments under different scenarios are set up respectively to prove the work of the proposed fault diagnosis model.

3.1 Fault sample generation analysis

The study was complemented by the Glow model to generate some new fault samples in different scenarios. For the purpose of demonstrating the work of the generated model, we used image quality metrics such as maximum mean difference (MMD) (Xu et al., 2018), peak signal-to-noise ratio (PSNR) (Wang et al., 2008), and feature similarity (FSIM) (Zhang et al., 2011) to value the validity of the generated fault samples. MMD can be used to judge the distribution difference between two images by using the size of the summation obtained from each image projection, and the smaller value indicates the smaller image distribution difference. PSNR is based on the relative value of the mean square error of the original sample and the generated sample and the square of the possible maximum signal value of the sample, and a higher value of PSNR indicates a higher quality of the generated sample. FSIM can be used to evaluate the image quality by using feature similarity, and higher values indicate better similarity.

Table 2 shows the quality evaluation of the generated fault samples with different noise intensities. Based on the magnitude of the 3 metrics, the original fault samples generated by the Glow model have better image quality than the generated noisy fault samples. The generated drive end fault samples have better image quality compared to the wind turbine bearing fan end fault samples. In the comparison of different image quality metrics, we find no significant degradation in the generated sample quality in the presence of noise interference. The experimental effect demonstrates that the proposed method has good performance to generate wind turbine bearing fault samples.

The study supplemented the number of wind turbine bearing fault samples in different scenarios by VAE, GAN, and Glow models, respectively. To verify the performance of the generated models, we used the image quality metrics above to evaluate the authenticity of the generated fault samples.

Table 3 shows the evaluation of the quality of the generated fault samples with different noise intensities. According to the magnitude of the three metrics, the Glow model supplemented generated fault samples have smaller differences and distortions compared to the fault samples generated by other models, and the samples are not as similar as several other models. The image quality of the drive-side fault samples generated by each deep learning generation model is better compared to the wind turbine bearing fan end fault samples.

3.2 Case analysis of sample imbalance scenario

Because the real fault probability is relatively low, the probability of each type of fault of the wind turbine bearing is also different, and the number of samples obtained for each fault category is also different. Therefore, in the actual fault diagnosis of the fan spindle, there will be a problem of unbalanced number of fault category samples. To address this problem, this paper uses Glow model to generate new samples based on 2 sets of wind turbine bearing vibration data respectively to supplement the sample number of unbalanced fault categories, and the fault sample sets with balanced sample number are used to get the diagnostic results through the multiple input bearing fault diagnosis model. The unbalanced fault sample set is shown in Tabel 4, where the sample number of balanced category is

2000 per category and the sample number of unbalanced category is 1,000 per category.

Figure 6 demonstrates the diagnostic results of different sample sets under sample imbalance scenario. When the sample imbalance is relatively low, the model can 100% accurately diagnose the faults. As the sample imbalance increases, the diagnostic effect of the model can decrease slightly. However, the model can still effectively diagnose wind turbine bearing faults, indicating that the new model has good bearing fault diagnosis ability under sample imbalance scenario.

3.3 Case analysis of sample shortage scenario

In the actual operation of the wind turbine, the collection of fault samples is very difficult, and the limited number of fault samples may affect the effect of fault diagnosis. For the purpose of confirming the fault diagnosis effect of the new method in complex scenarios, we construct sample sets based on different sample number and supplement the sample number through the Glow model until the sample number in the sample set is the same. The diagnostic effect of the proposed method is tested on the same sample set. The sample number in different sample sets is shown in Table 4.

Figure 7 shows the diagnostic results of the original sample set and the supplemental sample set in the scenario of insufficient samples. As shown in the figure, insufficient samples will lead to a decrease in the fault diagnosis effect of the sample set. The diagnostic result is better when the fault sample set is supplemented by the generative model. Although the diagnostic effect of the sample set with deep learning generation model supplemented with fault samples is not good enough, it also verifies that the new fault diagnosis method has certain effect when the samples are insufficient, and the fault samples generated by Glow model can effectively enhance the diagnostic accuracy.

3.4 Noise scenario experimental analysis

The study considers that the acquisition of vibration data in the wind generator operation may be disturbed by noise. For the purpose of proving the validity of the proposed fault diagnosis method in practical applications, the study simulates the noise scenarios in the actual operation by adding Gaussian white noise with different intensities to the sample data. The sample sets with different noise intensities are set by the original fault samples and the fault samples with different noise intensities according to Tables 3, 5.

Figure 8 is the diagnostic result of different sample sets under noise interference. When the fault samples are balanced and sufficient, the diagnostic result of the sample set is significantly better than that of other sample sets. When the samples are insufficient and unbalanced, the fault diagnosis effect of the sample set will decrease. The diagnosis accuracy of each sample set under special scenarios is relatively low, but the diagnosis accuracy of each sample set is above 97.5%. The study shows that the proposed model has good performance of the bearing fault diagnosis under the noise scenario.

3.5 Comparative experimental analysis

The combination of deep generative models and fault classification methods has the ability to solve unbalanced sample problems and small sample problems. In order to verify the ability of different deep learning generative models in complex scenarios fault recognition, this section compares the accuracy of fault diagnosis by supplementing the fault samples generated by different deep generative models, trained with the same sample set in the wind turbine bearing multi-signal input model.

Figure 9 shows the fault diagnosis accuracies of different deep generative models on the same sample set. In the unbalanced sample set, the fault diagnosis accuracy of the supplemental sample set of different deep learning generative models is basically the same. However, in the small sample set, the diagnostic accuracy of the fault sample set supplemented by the GLOW model is significantly higher than the diagnostic accuracy of the fault sample set supplemented by other deep learning generation models. In order to more intuitively reflect the superiority of GLOW, we have provided the average fault diagnosis accuracy of different models in the last column of Figure 9. The results show that the average diagnostic accuracy of GLOW model is significantly higher than that of the other two models. The experiments prove that the GLOW model has good performance in solving the unbalanced sample problem and the small sample problem in the multi-input fault diagnosis of wind turbine bearings.

4 Conclusion

In this study, the Glow model is used to learn the fault characteristics of each fault category to generate fault samples to enhance fault diagnosis accuracy under the scenario of insufficient fault samples and unbalanced sample number of different fault categories, and a multi-input fault diagnosis model is established to realize multi-category fault diagnosis at multiple locations of the wind turbine bearing. The experimental effect under different scenarios verifies the work of the proposed method. The proposed method can be applied in practice to improve the economic efficiency.

Data availability statement

The original contributions presented in the study are included in the article/Supplementary Material, further inquiries can be directed to the corresponding author.

Author contributions

BW: Conceptualization, Investigation, Writing–original draft. FW: Data curation, Formal Analysis, Methodology, Writing–original draft. YZ: Software, Writing–review and editing. SF: Resources, Software, Supervision, Writing–review and editing. HL: Validation, Visualization, Writing–review and editing. LZ: Funding acquisition, Project administration, Writing–review and editing.

Funding

The author(s) declare that no financial support was received for the research, authorship, and/or publication of this article.

Acknowledgments

Thank you to the authors for your contribution to this study, which could not have been achieved without your perfect cooperation.

Conflict of interest

Authors BW, FW, YZ, and SF were employed by State Power Investment Corporation Anhui Electric Power Co Ltd.

The remaining authors declare that the research was conducted in the absence of any commercial or financial relationships that could be construed as a potential conflict of interest.

Publisher's note

All claims expressed in this article are solely those of the authors and do not necessarily represent those of their affiliated organizations, or those of the publisher, the editors and the reviewers. Any product that may be evaluated in this article, or claim that may be made by its manufacturer, is not guaranteed or endorsed by the publisher.

Supplementary material

The Supplementary Material for this article can be found online at: https://www.frontiersin.org/articles/10.3389/fenrg.2023.1342811/full#supplementary-material

References

Chen, J., Pan, J., Li, Z., Zi, Y., and Chen, X. (2016). Generator bearing fault diagnosis for wind turbine via empirical wavelet transform using measured vibration signals. *Renew. Energy* 89, 80–92. doi:10.1016/j.renene.2015.12.010

Dinh, L., Krueger, D., and Bengio, Y. (2014). Nice: non-linear independent components estimation. arXiv preprint arXiv:1410.8516.

Dinh, L., Sohl-Dickstein, J., and Bengio, S. (2016). Density estimation using real nvp. arXiv preprint arXiv:1605.08803.

Fang, X., Xie, L., and Li, X. (2023). Distributed localization in dynamic networks via complex laplacian. *Automatica* 151, 110915. doi:10.1016/j.automatica.2023.110915

Heling, Y., and Yan, X. (2020). Preventive-corrective coordinated transient stability dispatch of power systems with uncertain wind power. *IEEE Trans. Power Syst.* 35 (5), 3616–3626. doi:10.1109/tpwrs.2020.2972003

Huang, N., Chen, Q., Cai, G., Xu, D., Zhang, L., and Zhao, W. (2020). Fault diagnosis of bearing in wind turbine gearbox under actual operating conditions driven by limited data with noise labels. *IEEE Trans. Instrum. Meas.* 70, 1–10. doi:10.1109/tim.2020.3025396

Kingma, D. P., and Dhariwal, P. (2018). "Glow: generative flow with invertible 1x1 convolutions," in *Advances in neural information processing systems 31* (NeurIPS).

Liu, Z., Yang, B., Wang, X., and Zhang, L. (2021). Acoustic emission analysis for wind turbine blade bearing fault detection under time-varying low-speed and heavy blade load conditions. *IEEE Trans. Industry Appl.* 57, 2791–2800. doi:10.1109/tia.2021.3058557

Loparo, K. (2012). Case western reserve university bearing data centre website. 2021-11-17). Avaliable at: http://engineering.case.edu/bearingdatacenter/download-data-file.

Pu, Z., Li, C., Zhang, S., and Bai, Y. (2020). Fault diagnosis for wind turbine gearboxes by using deep enhanced fusion network. *IEEE Trans. Instrum. Meas.* 70, 1–11. doi:10.1109/tim.2020.3024048

Rezende, D., and Mohamed, S. (2015). Variational inference with normalizing flows. arXiv.

Salimans, T., and Kingma, D. P. (2016). "Weight normalization: a simple reparameterization to accelerate training of deep neural networks," in *Advances in neural information processing systems 29* (Barcelona, Spain: NIPS).

Shiyao, Q., Chen, Q., and Shaolin, L. (2023). Review of the voltage-source grid forming wind turbine. *Proc. CSEE* 43, 1314–1334. doi:10.13334/j.0258-8013.pcsee.222095

Song, W., Lin, J., Zhou, F., Li, Z., Zhao, K., and Zhou, H. (2022). Wind turbine bearing fault diagnosis method based on an improved denoising AutoEncoder. *J. Power Syst. Prot. Control* 50, 61–68. doi:10.19783/j.cnki.pspc.210939

Su, Y., Meng, L., Kong, X., Xu, T., Lan, X., and Li, Y. (2022). Generative adversarial networks for gearbox of wind turbine with unbalanced data sets in fault diagnosis. *IEEE Sensors J.* 22, 13285–13298. doi:10.1109/jsen.2022.3178137

van de Schaft, V., and van Sloun, R. J. (2021). Ultrasound speckle suppression and denoising using MRI-derived normalizing flow priors. arXiv preprint arXiv:2112.13110.

Wang, X., Tang, G., Yan, X., He, Y., Zhang, X., and Zhang, C. (2021). Fault diagnosis of wind turbine bearing based on optimized adaptive chirp mode decomposition. *IEEE Sensors J.* 21, 13649–13666. doi:10.1109/jsen.2021.3071164

Wang, Y., Liu, W., and Wang, Y. (2008). Image quality assessment based on local variance and structure similarity. *J. Optoelectron. Laser* 19, 1546–1553. doi:10.16136/j.joel.2008.11.021

Xiao, X., Wang, J., Zhang, Y., Guo, Q., and Zong, S. Y. (2019). A two-dimensional convolutional neural network optimization method for bearing fault diagnosis. *Proc. CSEE* 39, 4558–4567. doi:10.13334/j.0258-8013.pcsee.182037

Xu, Q., Huang, G., Yuan, Y., Guo, C., Sun, Y., Wu, F., et al. (2018). An empirical study on evaluation metrics of generative adversarial networks. arXiv preprint arXiv:1806.07755.

Yongsheng, Q., Chengcheng, S., Shengli, G., Liqiang, L., and Chaoyi, D. (2022). FAULT DIAGNOSIS STRATEGY OF WIND TURBINES BEARING BASED ON AEWT-KELM. *Acta Energiae Solaris Sin.* 43, 281. doi:10.19912/j.0254-0096.tynxb.2020-1321

Yu, X., Tang, B., and Zhang, K. (2021). Fault diagnosis of wind turbine gearbox using a novel method of fast deep graph convolutional networks. *IEEE Trans. Instrum. Meas.* 70, 1–14. doi:10.1109/tim.2020.3048799

Zhang, J., Zhang, J., Zhong, M., Zheng, J., and Li, X. (2020). Pso-VMD-MCKD based fault diagnosis for incipient damage in wind turbine rolling bearing. *J. Vib. Meas. Diag* 40, 287–296. doi:10.16450/j.cnki.issn.1004-6801.2020.02.011

Zhang, L., Zhang, L., Mou, X., and Zhang, D. (2011). FSIM: a feature similarity index for image quality assessment. *IEEE Trans. Image Process.* 20, 2378–2386. doi:10.1109/tip.2011.2109730

Zhang, M., Li, C., and Zhou, Z. (2021b). Text to image synthesis using multi-generator text conditioned generative adversarial networks. *Multimedia Tools Appl.* 80, 7789–7803. doi:10.1007/s11042-020-09965-5

Zhang, T., Chen, J., Xie, J., and Pan, T. (2021a). SASLN: signals augmented self-taught learning networks for mechanical fault diagnosis under small sample condition. *IEEE Trans. Instrum. Meas.* 70, 1–11. doi:10.1109/tim.2020.3043098

Zheng, X., Chen, G., Ren, H., and Li, D. (2019). Fault detection of vulnerable units of wind turbine based on improved VMD and DBN. *J. Vib. Shock* 38, 153–160. doi:10.13465/j.cnki.jvs.2019.08.023